

## Macroscopic evidences for non-Rice-Ramsperger-Kassel effects in the reaction between $\text{H}_3\text{O}^+$ and $\text{D}_2\text{O}$ : The occurrence of nonstatistical isotopic branching ratio

Massimo Mella<sup>a)</sup>

*School of Chemistry, Cardiff University, Main Building, Park Place, Cardiff CF10 3AT, United Kingdom*

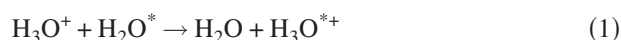
(Received 8 December 2006; accepted 27 April 2007; published online 23 May 2007)

The dynamics of the isotopic scrambling in the energized and metastable complex  $\text{D}_2\text{O}-\text{H}_3\text{O}^+$  has been studied using classical molecular dynamics (MD) trajectories starting from regions of phase space corresponding to an already formed collisional complex. The simulations cover the range of internal energies spanned by gas phase collision experiments. Rate constants for the isotopic exchange and the complex dissociation have been computed; the isotopic branching ratio  $\mathcal{R} = [\text{HD}_2\text{O}^+]/[\text{H}_2\text{DO}^+]$  has also been obtained from MD simulations and found to deviate substantially from an equivalent prediction based on a previously proposed kinetic scheme. This finding suggests the possibility that details of the reaction dynamics play a role in defining the isotopic branching ratio. The analysis of trajectory results indicated a relatively long lifetime for the collisional complex and the presence of multiple time scales for the exchange process, with a large fraction of the exchange events being separated only by a single oxygen-oxygen vibration or half of it. The occurrence of these fast consecutive jumps and their different probabilities as a function of the relative direction between first and second jumps suggest the presence of ballistic motion in the complex following each reactive event. This can be explained on the basis of overlapping regions in phase space and it is used to provide an explanation of the difference between kinetic and MD branching ratios. © 2007 American Institute of Physics. [DOI: 10.1063/1.2742381]

### INTRODUCTION

Energized polyatomic systems may present complicated reaction dynamics defying the assumptions of the statistical theories often employed for their analysis.<sup>1</sup> When searching for evidences of nonstatistical behavior, chemists have usually looked for slow energy exchange between modes [the intrinsic non-Rice-Ramsperger-Kassel-Marcus (RRKM) behavior described by Hase and co-workers<sup>2,3</sup> and experimentally substantiated by the work of Gruebele and co-workers<sup>4,5</sup>] and ballistic motion analyzing product energy distributions or the effects of mode specific excitations. Alternatively, one may observe unexpected branching ratios, e.g., a nonstatistical amount of products presenting an inverted configuration following a<sup>1,3</sup> sigmatropic migration.<sup>6</sup> In this specific case, the consequences of ballistic dynamics have been investigated experimentally,<sup>7</sup> with results supporting the original theoretical analysis<sup>6</sup> based on “on the fly” molecular dynamics (MD) trajectories.

A class of reactions that may present substantial nonstatistical effects due to the energized nature of intermediate species (i.e., collisional complexes) is provided by gas phase ligand exchanges. Within this class, the fundamental transformation



has been investigated in the past as prototypical ligand exchange reaction.<sup>8-13</sup> Despite the simplicity of the system, the

details of the internal dynamics of this process are still controversial. Indeed, evidences were given for both a long-lived complex, which may allow statistical scrambling of all protons<sup>8,10,11</sup> and a direct “stripping” mechanism,<sup>9</sup> which would instead prevent the scrambling. Using  $\text{D}_2\text{O}$  as a marker, recent single-collision experiments<sup>12,13</sup> provided strong evidences for a lack of statistical scrambling even at low collisional energies. In particular, the product branching ratio  $\mathcal{R} = [\text{HD}_2\text{O}^+]/[\text{H}_2\text{DO}^+]$  was found to be larger than expected from statistical considerations alone. Bearing in mind that  $\text{HD}_2\text{O}^+$  is the only possible detectable product of a stripping mechanism, the larger than statistical  $\mathcal{R}$  values may have been used as an indication of the importance of such process. Contradicting this assumption, a RRKM analysis carried out in Ref. 13 (see the process energy landscape in Fig. 1) suggested, instead, that these may be explained by means of the competition between the scrambling process and the complex dissociation (see Fig. 2). In other words, it was suggested that the dissociation rate constant ( $k_{\text{diss}}$ ) for the collisional complex was of the same order of magnitude of the scrambling rate ( $k_{\text{exch}}$ ), so that the system does not have enough time for a complete randomization of the isotopic distribution before breaking up. In the analysis carried out in Ref. 13,  $k_{\text{diss}}$  and  $k_{\text{exch}}$  are, respectively, defined as the rate constants for the two processes



and

<sup>a)</sup>Electronic mail: mellam@cardiff.ac.uk

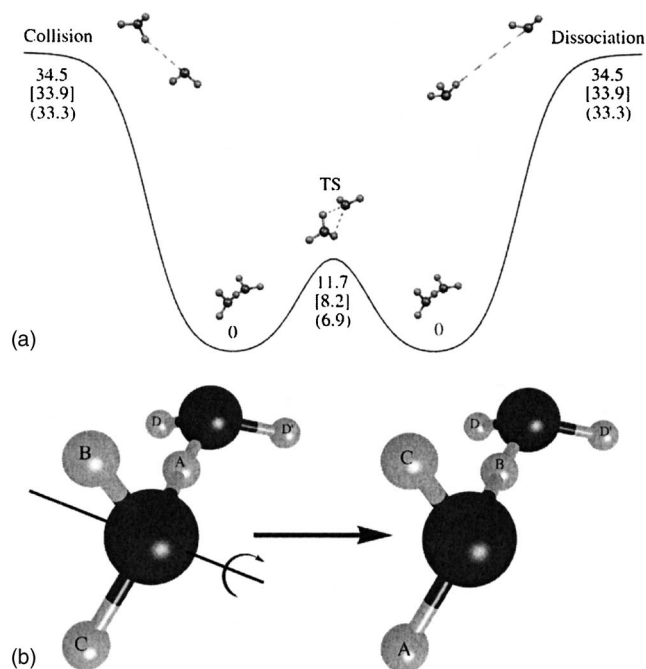


FIG. 1. Process involved during the  $\text{H}_2\text{O}-\text{H}_3\text{O}^+$  collision. (a) Potential energy surface (kcal/mol; MP2/aug-cc-pVTZ; OSS3, square brackets; OSS2 bracket). (b) Details of the pseudorotation inducing the proton exchange in the Zundel cation and choice of labels for the H atoms involved in the process. The process shown in this panel can be represented using the shorthand notation  $A \rightarrow C \rightarrow B \rightarrow A$ , where  $X \rightarrow Y$  means atom  $X$  moves in location previously occupied by atom  $Y$ .



where  $[\text{H}_5\text{O}_2^\ddagger]^\ddagger$  represents the metastable complex and the bridging  $\text{H}^*$  swaps its position with one of the external hydrogen atoms, here indicated as  $\text{H}^\dagger$  (see also Fig. 1 and the scheme of Fig. 2). A direct consequence of the idea presented in Ref. 13 is that the production of  $\text{HD}_2\text{O}^+$ , a fraction of which may come from the bridging proton randomly attaching itself during dissociation to the oxygen carrying the two deuteriums, may be favored at the expense of  $\text{H}_2\text{DO}^+$ . The latter necessitates, instead, of atomic scrambling to be produced. Noteworthy, the RRKM analysis<sup>13</sup> suggested the low-

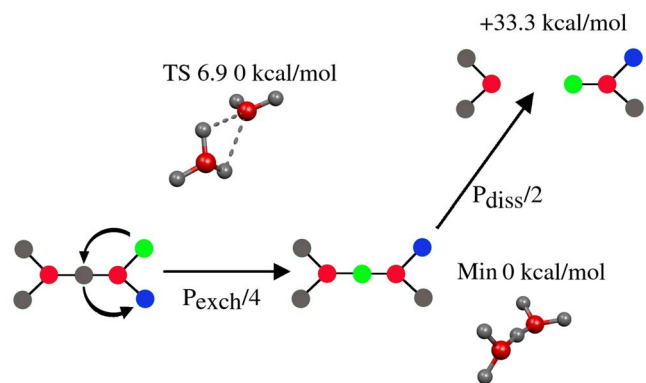


FIG. 2. Schematic representation of the exchange and dissociation processes in the Zundel cation. Red atoms are oxygens, gray atoms are hydrogens, and blue/green atoms are deuteriums. In the kinetic Monte Carlo scheme,  $P_{\text{exch}} = k_{\text{exch}} / (k_{\text{exch}} + k_{\text{diss}})$  and  $P_{\text{diss}} = k_{\text{diss}} / (k_{\text{exch}} + k_{\text{diss}})$ . The “ball and stick” models represent the minimum energy structure (min) and the transition state (TS) for the exchange process.

energy  $\mathcal{R}$  to be 1.4 times larger than the value (0.5) predicted using statistical consideration alone.

Underpinning the RRKM analysis in Ref. 13, there is, however, the assumption of statistical behavior for the collisional complex  $\text{H}_3\text{D}_2\text{O}_2^+$ . In this respect, the large amount of internal energy in the collisional  $\text{H}_3\text{D}_2\text{O}_2^+$  and the presence of identical equilibrium structures connected by means of a pseudorotation of a hydronium moiety [Fig. 1(b)] suggest that nonstatistical effects may be important in the process. Moreover, recent theoretical investigations<sup>14,15</sup> provided evidences for a relatively long complex lifetime ( $\sim 10$  ps) at low energy. This finding supports the idea of a long lasting species and, hence, of the likelihood of statistical H/D scrambling. It is therefore the aim of this work to investigate the impact of assuming statistical behavior on the description of the processes taking place after a collision between  $\text{H}_3\text{O}^+$  and  $\text{H}_2\text{O}$  (or  $\text{D}_2\text{O}$ ). In this respect, MD trajectories and statistical simulations<sup>15</sup> can be used to study the internal dynamics and to compute reaction rates for the  $\text{H}_5\text{O}_2^+$  complex. To do so, the OSS2 and OSS3 models<sup>16</sup> were chosen as potential energy surfaces (PESs) for  $\text{H}_5\text{O}_2^+$ , these models being found to accurately reproduce the dissociation energy of the complex [see Fig. 1(a)] and to provide an accurate description of the barriers separating isomeric structure in larger clusters.<sup>17</sup> The differences between the two models were used to investigate the sensitivity of the results to the details of the PESs.

## METHODS AND RESULTS

### Calculation of reaction rate constants and branching ratios using MD and statistical theories

As first step in our investigation, values for  $k_{\text{diss}}$  and  $k_{\text{exch}}$  were computed as a function of the total internal energy  $E_{\text{int}}$  using MD simulations<sup>19</sup> and a new implementation<sup>15</sup> of the efficient microcanonical sampling transition state theory (EMS-TST).<sup>20</sup> In all calculations, it was assumed that a “loose complex” having a lifetime long enough to define a meaningful dissociation rate was formed as a result of the collision between  $\text{H}_3\text{O}^+$  and  $\text{H}_2\text{O}$  (or  $\text{D}_2\text{O}$ ). For every energy investigated, 20 000 trajectories were started with random initial momenta and positions sampled accordingly to the proper microcanonical distribution of the adduct intermediate (i.e., constant total internal energy  $E = E_{\text{vib}} + E_{\text{rot}}$ ), using the EMS method as described in Ref. 20. Noteworthy, the EMS method does not allow one to easily select a specific total angular momentum ( $J$ ) for systems of the size of the Zundel cation. Thus, the dependency on  $J$  of the rate constants and other properties can only be extracted *a posteriori* analyzing the trajectory results. This analysis can be carried out coarse-graining the total angular momentum distribution  $P(J)$ , provided the sample of trajectory initial conditions is sufficiently large. Figure 3 shows the probability distribution function for  $J$  sampled at the lowest, an intermediate, and highest energy used in the Monte Carlo microcanonical simulations.

Each trajectory was run for 10 ps or until dissociated. A trajectory was considered dissociated when the distance between the two oxygens was larger than 15 a.u. In every case,

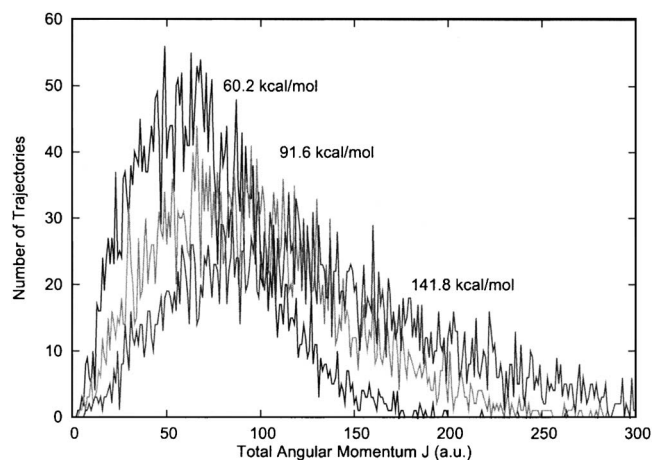


FIG. 3. Distribution of the number of trajectories with a specific total angular momentum  $J$  (in a.u.) sampled during the Monte Carlo EMS simulations at three different energies.

dissociation rates were computed assuming a first order dissociation law and fitting the time dependence of  $\ln[(N_0 - N_t)/N_0]$  with a straight line. Here,  $N_0$  is the total number of trajectories and  $N_t$  is the number of trajectories dissociated at time  $t$  (angular momentum resolved rate constants can be obtained with the same procedure selecting values of  $J$ ). Exchange rates, instead, were computed using MD simulations as  $k_{\text{exch}} = 1/\tau$ , where  $\tau$  is the average gap time between two subsequent exchange events. To define the latter, the identity of bridging proton was assigned to the H atom with the lowest value of the coordinate  $\mu_i = r_{i,1} + r_{i,2}$ , where  $r_{i,k}$  is the distance between the  $i$ th hydrogen and the  $k$ th oxygen. The same reaction coordinate was used to predict statistical rates for the exchange process.

The rate constants obtained from the complete set of trajectories using the OSS2 model are shown in Fig. 4 for a range of internal energies ( $E_{\text{int}}$ ) spanning from roughly 60 kcal/mol, well above the complex zero point energy (ZPE) (37.4 kcal/mol),<sup>18</sup> to 145 kcal/mol (see EPAPS for Supplementary Material providing tables of results obtained also with OSS3).<sup>21</sup> A similar range was covered by collision experiments.<sup>13</sup> Figure 5 shows the total angular momentum-

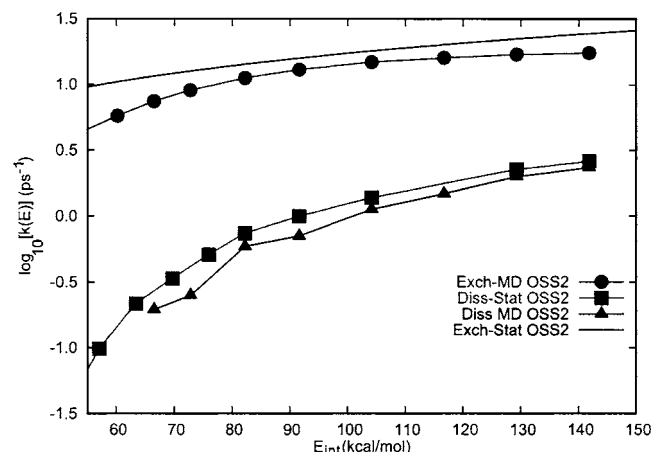


FIG. 4. Logarithm of the rate constants ( $\text{ps}^{-1}$ ) vs  $E_{\text{int}}$  (kcal/mol) for the exchange (exch) and dissociation (diss) processes computed with MD simulations and statistical theories (stat) on the OSS2 surface.

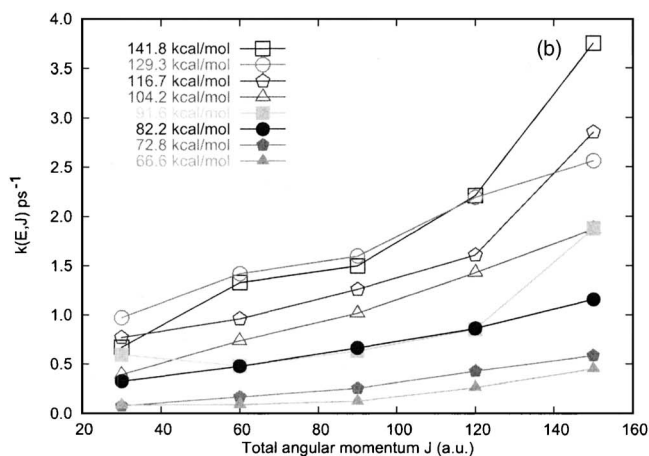
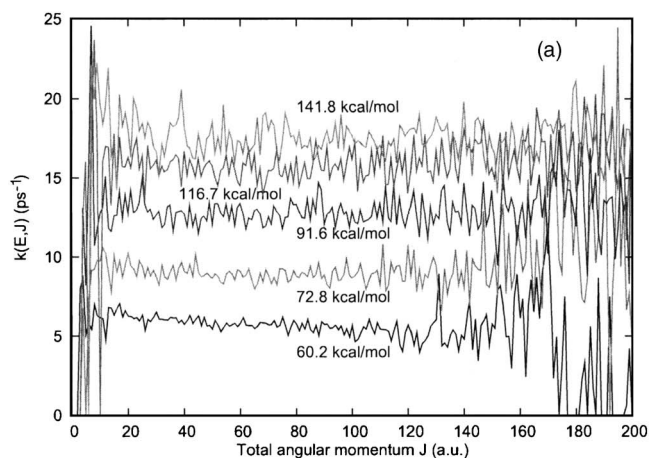


FIG. 5. Angular momentum-resolved rate constants  $k(E, J)$  for the exchange (a) and dissociation (b) processes as a function of the angular momentum  $J$  for different energies (OSS2 PES). The values of  $J$  have been coarse grained using bin width of 1 and 4 a.u. of  $J$  for exchange and dissociation, respectively.

resolved exchange ( $k_{\text{ex}}(E, J)$ ) and dissociation rates ( $k_{\text{diss}}(E, J)$ ), obtained coarse-graining the values of  $J$  over intervals of  $\pm 0.5$  and  $\pm 2$  a.u., respectively. As for the exchange rate [Fig. 5(a)], it is clearly seen that this depends only weakly on the total angular momentum of the trajectory, perhaps suggesting the lack of strong coupling between the internal exchange process and the rotational motion of the species. Differently, the dissociation rate is seen to increase, roughly, by a factor of 3–4 upon increasing the angular momentum of the trajectories.

Apart from the long surviving trajectories for which the sample was not sufficiently large to obtain statistically meaningful results, we found, in general, that  $\ln[(N_0 - N_t)/N_0]$  closely followed a linear behavior for every ensemble ( $E, J$ ) of dissociating trajectories. In turn, this indicates that the trajectory lifetime distribution

$$P(t) = -\frac{1}{N(0)} \frac{dN(t)}{dt} \quad (4)$$

for this process presents a RRKM-type behavior, i.e., the distribution closely follows the formula  $P(t) = k(E, J) \times \exp(-k(E, J)t)$  as predicted by RRKM theory [see Fig. 6(b) for an example]. Conversely, the shape of the lifetime distri-

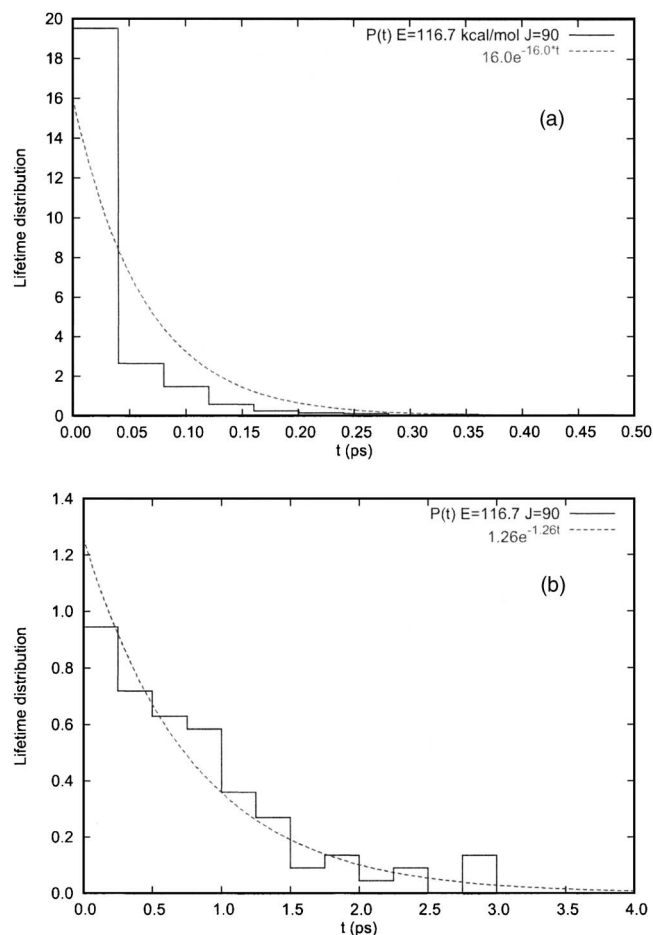


FIG. 6. Lifetime distribution for the exchange (a) and dissociation (b) processes for trajectories with  $E=116.7$  kcal/mol and  $J=90$ . The dashed curves represent the lifetime distribution obtained using the MD computed rate constant for the two processes.

tribution for the exchange process departs from the analytical prediction of RRKM theory, presenting a larger number of events happening at short time than predicted using the MD rate constants. We interpret this finding as a possible indication of nonstatistical behavior for the internal scrambling process, which warrants further investigation.

The comparison between MD and statistical dissociation rate constants indicates the latter to be similar or slightly higher than the former, and suggests a somewhat longer lifetime for  $\text{H}_5\text{O}_2^+$  than predicted by statistical theories. At the same time, we found that dissociation rate constants obtained analyzing only short-lived trajectories agreed (within 20%) with the results of microcanonical statistical theory. This finding indicates that the Monte Carlo (MC) simulations are successful in sampling the microcanonical ensemble. Similarly, the statistical estimate for  $k_{\text{exch}}$  gives values roughly 1.5 larger than the MD simulation counterpart, with the short time MD constants agreeing within 20% of the statistical rates. It is important to point out that the comparison between MD and statistical rates was made using statistical rate constants averaged over the sampled ensemble of initial  $J$  conditions (i.e., without resolving with respect to  $J$ ) as obtained with MC simulations. Unfortunately, this limitation is due to difficulties in defining a total angular momentum for the system during the statistical sampling.

Worth noticing, it is the fact that both approaches predict a high value for the  $\mathcal{K}=k_{\text{exch}}/k_{\text{diss}}$  ratio, the latter spanning from  $\sim 36$  (at low energy) to  $\sim 10$  (at high energy) for MD, and from  $\mathcal{K} \sim 32$  to  $\mathcal{K} \sim 11$ , respectively, for statistical simulations. These large values of  $\mathcal{K}$  are in agreement with the relative barrier heights [Fig. 1(a)] and suggest that several exchanges may take place before dissociation. They also support the possibility of an almost complete scrambling of protons and deuteriums, especially at low energy. It is, however, worth stressing that statistical rate theory provides somewhat lower values of  $\mathcal{K}$  than MD simulations, which may have an impact on the values of the branching ratio  $\mathcal{R}$ .

To test the possibility of complete scrambling in the complex, two new sets of MD simulations were run to obtain a theoretical prediction for  $\mathcal{R}$  using the same protocol discussed above. In the first set, two of the four nonbridging H atoms, both bound to the same oxygen (Fig. 2), were labeled as deuterium at the beginning of the trajectory but were given the H atomic mass. The second set, instead, was run giving the two “marked” hydrogens the correct value for the deuterium mass. In principle, this approach should allow one to extract information on the isotopic effect in the process; the branching ratio for both sets was obtained by analyzing trajectories that had dissociated within 10 ps.<sup>22</sup> As a way to extract the effect of the detailed dynamical treatment on the branching ratio of this reaction, the MD values for  $\mathcal{R}$  need to be compared with an equivalent prediction based on a kinetic model employing the  $J$ -ensemble averaged MD values for  $k_{\text{exch}}$  and  $k_{\text{diss}}$  obtained from the MC simulations. With this aim in mind, it was decided to use the reaction scheme proposed in Fig. 5 of Ref. 13, the latter being implemented using kinetic Monte Carlo (KMC) simulations,<sup>23</sup> in these, exchange and dissociation events were randomly selected with relative probability  $k_{\text{exch}}/k_{\text{diss}}$ . To simulate the effect of the exchange event, an external proton was randomly chosen to substitute the bridging one and the isotopic distribution updated as shown in Fig. 2. The KMC game was terminated whenever the dissociation event was selected; at that stage, the bridging proton (or deuteron) was randomly assigned to one oxygen and the products were analyzed to define their isotopic composition. Several iterations of this procedure allowed us to estimate the statistical error associated with the computed branching ratio.

The  $\mathcal{R}$  values computed using both trajectory and KMC simulations are shown in Fig. 7. As for the KMC results, we begin by noticing that  $\mathcal{R}$  remains quite low (0.55–0.77) over all the energy interval. In particular, the low-energy simulations predict an almost statistical value for the branching ratio (0.55 vs 0.50), a result in good agreement with the large  $\mathcal{K}$  ratio ( $\approx 36$ ). Clearly, several exchanges are allowed to take place before the dissociation event is selected, thus producing a nearly complete scrambling.  $\mathcal{R}$  increases gradually upon increasing the internal energy, a finding that is correlated to the monotonic decrease in  $\mathcal{K}$ . However,  $[\text{HD}_2\text{O}^+]/[\text{H}_2\text{DO}^+]$  remains quite small even at highest energy in spite of the fourfold decrease in  $k_{\text{exch}}/k_{\text{diss}}$ .

The trajectory results for  $\mathcal{R}$  are clearly at variance with the KMC data, the MD branching ratio presenting values always higher than its statistical counterpart. In particular,

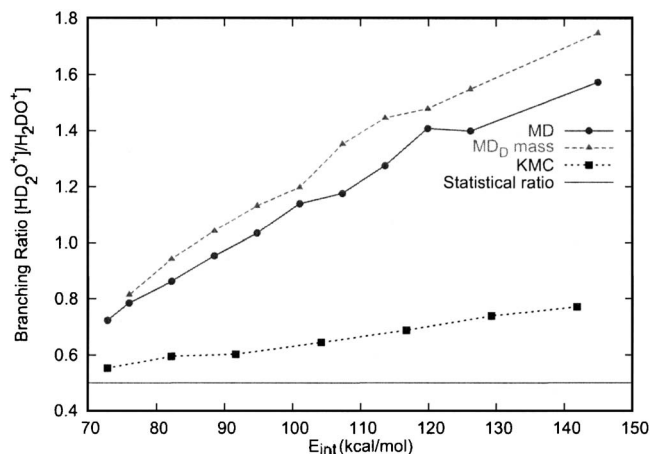


FIG. 7. Branching ratio  $[\text{HD}_2\text{O}^+]/[\text{H}_2\text{DO}^+]$  as a function of the internal energy of the Zundel cation. “MD<sub>D</sub> mass” and “MD” indicate results obtained using trajectories employ for H and D either the correct isotopic mass or, disregarding the difference, the proton mass for both. “KMC” indicates results obtained using kinetic Monte Carlo, whereas “statistical ratio” gives the statistical probability of dissociating in isotopically different species starting from a randomized  $\text{H}_3\text{D}_2\text{O}_2^+$ .

the value for  $\mathcal{R}$  obtained from low-energy simulations employing the hydrogen mass for both H and D is 0.72, which differs substantially from the KMC result (0.55) despite the large value of  $\mathcal{K}$ , and it is in excellent agreement with the extrapolated experimental data. It is important to stress, however, that a satisfactory comparison between our numerical data and the experimental results would require estimation of the collisional cross section between  $\text{H}_3\text{O}^+$  and  $\text{D}_2\text{O}$ , for which large impact parameters may be expected to play an important role due to the charge-dipole interaction. Nevertheless, the weak dependency of our MD rate constants on  $J$  suggests that, at least as first approximation, these simulation results may be used as guideline to interpret the experimental scrambling data.

A similarly large value for  $\mathcal{R}$  is obtained from the kinetic model only when  $\mathcal{K}=9$ , and this difference may be interpreted as a direct indication of the important role played by the actual dynamics in defining the macroscopic isotope distribution. It is also apparent that  $\mathcal{R}$  obtained using the MD simulations increases more steeply upon increasing  $E_{\text{int}}$ , than predicted by the KMC runs. Bearing in mind the distribution of  $J$  values sampled with the microcanonical MC simulations, this finding seems to suggest that additional factors, different from the competition between exchange and dissociation, may be playing a role in defining the relative amount of  $\text{HD}_2\text{O}^+$  and  $\text{H}_2\text{DO}^+$  produced. To test the robustness of this idea,  $\mathcal{R}$  values were recomputed using  $k_{\text{diss}}$  obtained from trajectories with  $J=60$  and  $J=90$ , two values of the total angular momentum sampled with high frequency by the MC simulations. In both cases, we found very similar trends, with only minor changes with respect to the results in Fig. 7.

Using the correct deuterium mass for the “marked” atoms is found to have only a small effect on  $\mathcal{R}$ , with results from the second set of simulations being shifted to slightly higher values. This shift is easily explained invoking a normal isotopic effect, with the rate constant for a deuterium

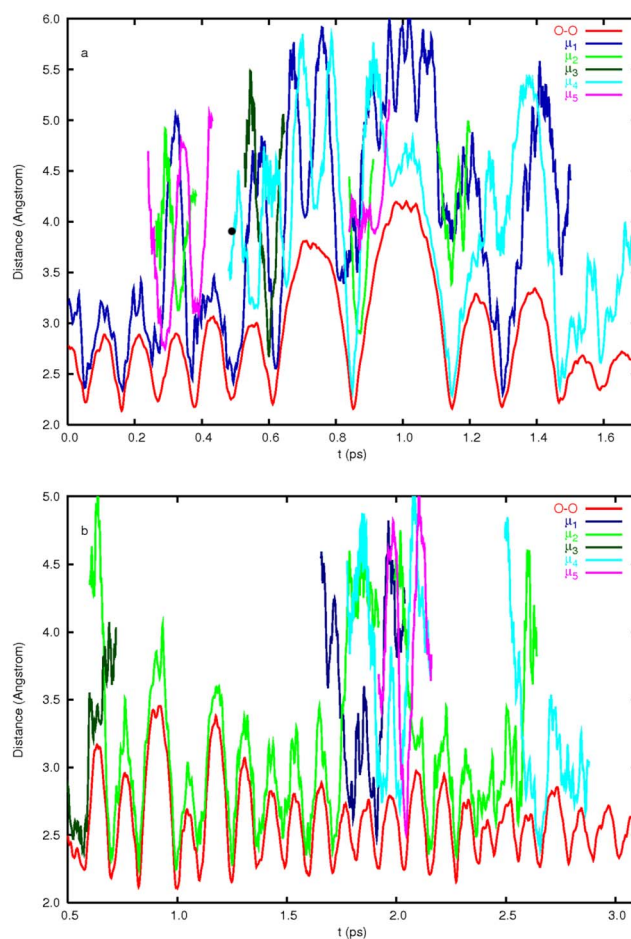


FIG. 8. Time evolution of the O–O distance and internal coordinates  $\mu_i$  for two representative trajectories with different values of  $E_{\text{int}}$ : (a) 82 and (b) 63 kcal/mol. To improve the clarity of the pictures, the oxygen–oxygen distance (lowest line, red) has been scaled by a factor of 0.95. For the same reason, some of the curves representing  $\mu_i$  for the protons are shown only in the vicinity of exchange events. The latter are defined as the time when  $\mu_i = \mu_j$  ( $i \neq j$ ), i.e., as the crossing time of two different  $\mu_i$  curves (different colors). Notice that exchanges happen primarily close to the outer or inner turning points of the oxygen–oxygen vibration, and that, upon increasing the energy, the frequency of two exchanges happening after a short time gap increases substantially, leading to more exchanges clustered together.

substituting the bridging atom being lower than in the case of a hydrogen due to a higher average velocity along the reaction coordinate in the latter case.

#### Detailed investigation of the Zundel internal dynamics using MD trajectories

Quite clearly, the substantial discrepancy between MD and KMC results for  $\mathcal{R}$  requires us to further investigate the details of the internal dynamics leading to both exchange and dissociation in the complex. To this end, a few hundred MD trajectories were visually inspected, the most striking features found being the occurrence of multiple consecutive exchange events (see Fig. 8 for two trajectories at different energies). To characterize quantitatively the phenomenon, the distributions of the delay time  $\Delta t$  between two consecutive exchanges were extracted from the simulations on  $\text{H}_5\text{O}_2^+$ , and these are shown in Fig. 9. In all cases, events with  $\Delta t$

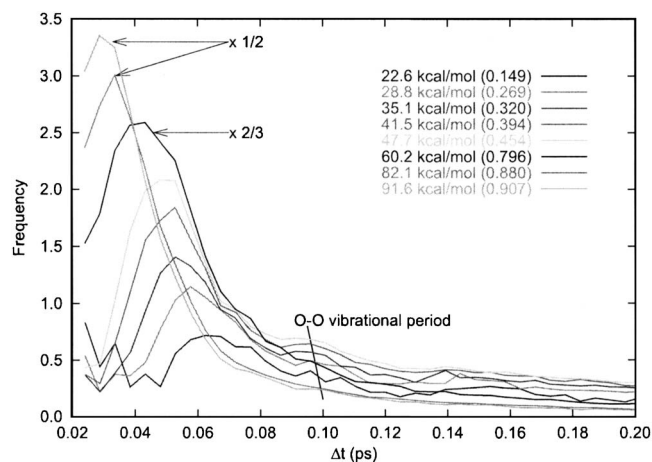


FIG. 9. Energy dependence of the delay time  $\Delta t$  (ps) probability for two consecutive exchanges obtained using the OSS2 potential. The numbers in brackets represent the fraction of exchange events with  $\Delta t \leq 0.12$  ps.

$\leq 0.02$  ps were neglected to eliminate instantaneous fluctuations (recrossing) along the reaction coordinate. The distributions present two main features, a tall maximum ( $\Delta t \sim 0.03$ – $0.06$  ps) and a broad peak ( $\Delta t \sim 0.09$ – $0.11$  ps), superimposed on a long exponential tail.<sup>21</sup> Comparing Fig. 9, Fig. 8, and movies of MD trajectories,<sup>21</sup> the two peaks were assigned to a second exchange happening after either half of or a complete oxygen-oxygen vibration, respectively. The exponentially decaying trend at longer time ( $\Delta t \geq 0.12$  ps) provides instead evidences for the presence of a process following closely a statistical behavior (i.e., of trajectories trapped for some time in the product well). Thus, the presence of three different time scales for the exchange process emerges from Fig. 9. Interestingly, the MD results indicate that the fraction of two consecutive exchanges separated by less than 0.12 ps is quite large even at low energy, and that it increases substantially upon increasing  $E_{\text{int}}$  (see legend in Fig. 9). At variance with fundamental transition state theory hypothesis, the analysis of MD trajectories also showed that exchanges happen primarily in the vicinity of the inner and outer turning points of the oxygen-oxygen vibration (see Fig. 8) rather than near the TS geometry. This suggests the picture of a dynamical process facilitated by trajectories straying away from the minimum energy path. Similar qualitative results are obtained using OSS3, indicating that changes in the PES details do not substantially modify the dynamical picture. We consider this insensitivity as a reflection of the relatively large amount of energy available to  $\text{H}_5\text{O}_2^+$  per degree of freedom.

Although providing robust evidence for the lack of statistical behavior in the exchange process, the findings just discussed do not suffice to explain the disagreement between KMC and MD branching ratios. This is easily understood by noticing that the complicated time gap distributions presented in Fig. 9 do not, in principle, indicate any symmetry breaking in the exchange process itself nor a change in the average number of scrambling events per trajectory. To investigate this matter further, the MD trajectories were reanalyzed separating the contributions to the exchange coming from dynamically nonequivalent protons [see Fig. 1(b) for

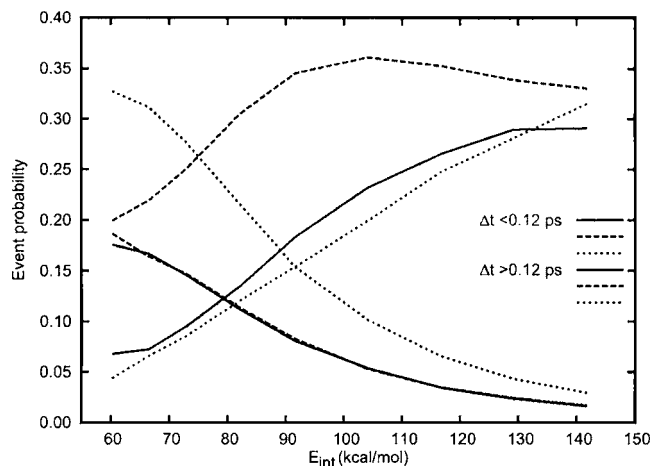


FIG. 10. Fraction of consecutive exchanges happening within (red) or after (blue) 0.12 ps. The solid lines represent a reverse rotation ( $B \rightarrow C \rightarrow A \rightarrow B$ ), the long dashed lines indicate a rotation in the same direction of the original exchange ( $B \rightarrow A \rightarrow C \rightarrow B$ ), and the short dashed lines are exchanges with protons  $D$  or  $D'$  [Fig. 1(b)].

our choice of labeling], thus extracting more detailed information about the mechanism and its dependence on the internal energy and delay time  $\Delta t$ . In particular, attention was focused to see if a particular nonbridging proton (or better a particular proton location in the system) was more likely to be involved in a second exchange event. To clarify this idea, let us suppose that an initial event has taken place as represented in Fig. 1(b), i.e., via the pseudorotation  $A \rightarrow C \rightarrow B \rightarrow A$ . Then, a second event may take place continuing the same motion (i.e., via the “direct” pseudorotation  $B \rightarrow A \rightarrow C \rightarrow B$ ), via an “inverse” rotation ( $B \rightarrow C \rightarrow A \rightarrow B$ ), or exchanging either protons  $D$  or  $D'$  with the bridging  $B$  ( $D \rightarrow B$  and  $D' \rightarrow B$ , respectively). Given the qualitative change in behavior shown by the distribution of delay time around  $\Delta t = 0.12$  ps (Fig. 9), the contributions due to events happening before or after  $\Delta t = 0.12$  ps were separately accumulated. However, it is important to point out that this operational choice does not guarantee a complete separation between statistical and nonstatistical events, especially when  $\Delta t \leq 0.12$  ps. Indeed, the two mechanisms are likely to be overlapping in this time range (statistical jumps may also happen after short time gaps), so that the proposed partitioning has to be considered only as a rough guide of their relative occurrence. The results of this analysis are presented in Fig. 10 as a function of  $E_{\text{int}}$ , with the contributions due to the  $D \rightarrow B$  and  $D' \rightarrow B$  processes added together. As a first observation, we notice that the relative probabilities for the three sets of events when  $\Delta t \geq 0.12$  ps are consistent with statistical theories, the latter predicting the observed 1:1:2 frequency ratio for the direct, inverse, and  $D \rightarrow B$  plus  $D' \rightarrow B$  processes, respectively. The lack of structure in the time gap distribution (Fig. 9) for  $\Delta t \geq 0.12$  ps also suggests that there is no correlation between two subsequent events happening after the time needed for a complete O–O vibration, a finding in line with the prediction of statistical theories. Noteworthy, the total fraction of all reactive events taking place with  $\Delta t \geq 0.12$  ps decreases quickly upon increasing the energy, as suggested by the results shown in Fig. 9.

For  $\Delta t \leq 0.12$  ps, instead, the relative frequencies of the three sets of processes are clearly nonstatistical and apparently dominated by the direct pseudorotation. The latter is seen to increase in frequency upon increasing  $E_{\text{int}}$ , a trend that can be understood using the concept of “transitional regions” in phase space. This was introduced in a model proposed by Carpenter<sup>24</sup> to discuss the nonstatistical effects in thermal reactions involving reactive intermediates sitting in shallow minima of the PES, and it is reminiscent of the idea of bottleneck in phase space proposed by Cho *et al.*<sup>25</sup> In both cases, the energy accumulated in some important set of molecular modes is not quickly exchanged with the remaining ones, so that the randomization of the phase space occupancy is severely hampered. When applied to the specific case of the intermediate adduct formed by  $\text{D}_2\text{O}$  and  $\text{H}_3\text{O}^+$ , a “transitional region”  $\Omega$  is the volume of phase space occupied by trajectories that either have just (timewise) entered the channel of the exchange products ( $\Omega_P$ ) after having surmounted the barrier, or that will be undergoing the exchange process within some (small) amount of time ( $\Omega_R$ ). In this respect, the pseudorotational motion involved in the exchange event makes it likely for reactive trajectories that reached  $\Omega_P$  to overlap with  $\Omega_R^D$ , the volume of phase space occupied by the initial conditions of trajectories that will lead to another exchange in the same direction of pseudorotation. Bearing this in mind, the increase in the fraction of direct second events upon increasing  $E_{\text{int}}$  should be interpreted as an increase of the “width” of  $\Omega_R^D$ , in agreement with the original prediction of the phase space model.<sup>24</sup> A similar behavior is also seen for the other two processes, namely, the inverse and  $D \rightarrow B/D' \rightarrow B$  exchanges. In these cases, however, the conditional probability for these two events is found to be smaller than for the direct event at low  $E_{\text{int}}$ , suggesting a scarce overlap between regions in phase space. This, in turn, can be an indication of weak coupling between the pseudorotation of two different  $\text{H}_3\text{O}^+$  moieties or of the lack of a mechanism able to invert the angular velocity of the rotating  $\text{H}_3\text{O}^+$ . At large energy, the inverse event becomes almost as likely as the direct event, suggesting a similar overlap between transitional regions and the onset of a barrier in phase space capable of inverting the momentum along the reaction coordinate. This fact can be rationalized recognizing that the inner turning point of the O–O vibration shortens, in the average, upon increasing  $E_{\text{int}}$ , and that the energy barrier for the exchange process at shorter O–O distances is substantially higher than around the equilibrium geometry (Fig. 11). This increase in the barrier effectively provides a repulsive wall against which trajectories can “bounce,” thus inverting the direction of the rotation. The cumulative probability for both  $D \rightarrow B$  and  $D' \rightarrow B$  exchanges, instead, remains substantially lower than expected from statistical consideration alone, suggesting that the reaction dynamics maintains, to a good degree, its ballistic character over all energy range.

### The relationship between nonstatistical dynamics and branching ratio $\mathcal{R}$

The analysis carried out in the previous section has clearly highlighted the presence of strong nonstatistical be-

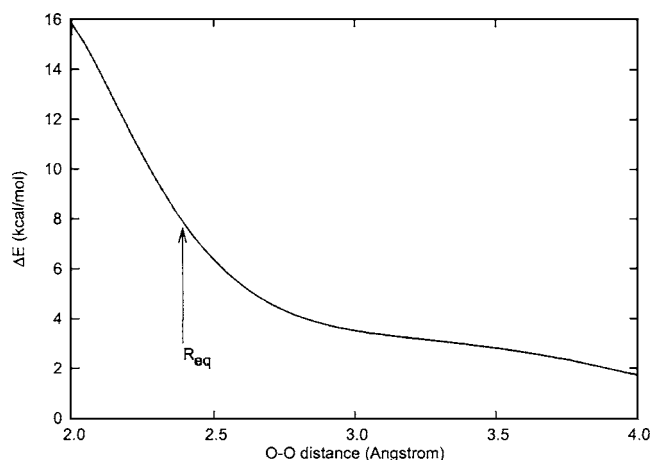


FIG. 11. Energy barrier for the pseudorotation of the  $\text{H}_3\text{O}^+$  moiety in the Zundel cation as a function of the O–O distance computed using the OSS2 potential.

havior in the internal dynamics of the Zundel cation, providing evidences for the possible failure of TST and of statistical reaction models in describing the exchange process. Bearing these results in mind, the aim of this section is to provide an explanation for the disagreement between KMC and MD values of the branching ratio  $\mathcal{R}$ . In this respect, the high values assumed at short time by the correlation function in Fig. 9 and the nonstatistical fractions of second jumps happening within  $\Delta t = 0.12$  ps direct us toward a possible way to rationalize the nonstatistical behavior (in the sense of the kinetic model) extracted from MD simulations. Let us start by stressing the fact that a cluster composed by two reactive events very close together (double jump) may need to be considered as a single reactive event, and that this may have somehow the effect of reducing the effective number of exchanges available to the Zundel cation before dissociation. This conclusion is true if the second correlated event is not randomly chosen among all possible ones, but instead subjected to preferential selection due to the presence of ballistic dynamics. To explain how this can actually work, it is of particular interest to consider a cluster of two events composed by an initial exchange (e.g.,  $A \rightarrow C \rightarrow B \rightarrow A$ ) followed by its inverse transformation (i.e.,  $B \rightarrow C \rightarrow A \rightarrow B$ ). This cluster alone accounts for two exchanges in the total exchange rate, but produces no impact at all on the isotopic distribution! Similarly, substituting the inverse second event with a direct one (i.e.,  $B \rightarrow A \rightarrow C \rightarrow B$ ) generates a cluster that also accounts for two reactive jumps but has the net effect of a single pseudorotation in the opposite direction [i.e.,  $A \rightarrow B \rightarrow C \rightarrow A$ , starting from the initial configuration in Fig. 1(b)]. The two remaining possibilities, i.e., clusters with either  $D \rightarrow B$  or  $D' \rightarrow B$  as final jumps, have no alternative interpretation, thanks to the fact that they allow a previously external hydrogen or deuterium to move to the opposite side of the system (on a different oxygen). Let us now suppose that the latter two clusters happen with zero frequency; in this case, only the cluster with a direct second jump would have any effect on the isotopic distribution due to the strict pairing of events. So, the effective number of transformations that could have an effect on the isotopic distribution

would be reduced by a factor of 2, with respect to the total number of pseudorotations, if the inverse second jump was never chosen, or by a factor of 4 if it was chosen with probability equal to the direct one. As a consequence of this analysis, it should become clear that, whenever the two clusters with  $D \rightarrow B$  or  $D' \rightarrow B$  as final jumps display a frequency lower than the one predicted by simple statistical arguments, i.e., lower than twice the frequency of double jumps with either a direct or inverse second jumps, the evolution of the isotopic distribution is likely to be slowed down compared to what would happen if every jump was subjected to statistical selection. This leads to an effectively lower value for  $\mathcal{K}_{\text{MD}}$  and a higher value for  $\mathcal{R}_{\text{MD}}$ . Bearing this analysis in mind, it is also straightforward to conclude that the effective rate constant for the exchange process must be somewhat reduced by an increase in the frequency of double jumps with direct and inverse second jumps with respect to  $D \rightarrow B$  and  $D' \rightarrow B$  events, and by a decrease in statistical jumps. These conclusions qualitatively agree with the behaviors shown in Figs. 9 and 10 by  $\mathcal{R}_{\text{MD}}$  and by the conditional probability for the second correlated jump, suggesting that  $\mathcal{R}_{\text{MD}}$  should always be expected to be higher than  $\mathcal{R}_{\text{KMC}}$ .

There is, however, another factor that needs to be taken into account to reach a quantitative understanding of the final value of  $\mathcal{R}$  obtained from the MD simulations. Indeed, the direct analysis of trajectories highlighted also the presence of clusters composed by three or more exchanges (very often three pseudorotations in the same direction), as shown in Fig. 5 (see also Ref. 21). The frequency of these multiple events was found to increase quickly upon increasing  $E_{\text{int}}$ . Bearing in mind the analysis carried out in the previous sections, it should be now clear that these larger aggregates may have an even deeper impact on the effective value of  $\mathcal{K}$  than two-jump clusters. Unfortunately, the extent of their impact on the final value of  $\mathcal{R}$  is difficult to estimate from the data provided in Fig. 6, a quantitative analysis of the fraction of multiple events as a function of  $E_{\text{int}}$  being necessary to correctly address the problem. This, however, would force one to compute the probability distribution function for the time gap of (at least) three consecutive events, a task expected to require a computational effort two orders of magnitude larger than that necessary to obtain the data presented in Figs. 9 and 10.

## CONCLUSIONS

MD trajectories were used to study the internal dynamics of the postcollisional complex formed by  $\text{H}_2\text{O}$  (or  $\text{D}_2\text{O}$ ) and  $\text{H}_3\text{O}^+$  starting from regions of phase space representing the adduct and spanning the range of energies explored by gas phase experiments. The substantial amount of internal energy per degree of freedom present in the collisional complex facilitates the occurrence of multiple exchange events separated only by half of or a complete O–O vibration and characterized by ballistic dynamics. At energies relevant for gas phase collision experiments (i.e.,  $70 \leq E_{\text{int}} \leq 140$  kcal/mol), the fraction of these events is fairly high (40% at least, see Fig. 9) compared with the exchanges presenting a more statistical behavior (i.e., an exponential distribution of delay

times). So, the trajectory results suggest the inability of RRKM theory to describe the process of isotopic scrambling induced by the collision between  $\text{D}_2\text{O}$  and  $\text{H}_3\text{O}^+$ .

The ballistic motion inherently present in the MD trajectories gives rise to a value of  $\mathcal{R}$  higher than obtained from KMC simulations employing MD-derived rate constants. So, caution should be exercised when analyzing the H/D exchange mechanism with a standard kinetic model based on the macroscopic/statistical idea of a time-independent reaction rate. Perhaps, the experimental data provided in Ref. 13 might need to be reinterpreted in light of the results of this work. In particular, it might prove to be necessary to extend the original idea of a competition between exchange and dissociation, also keeping into account the nonstatistical nature of the exchange process and its effect on the relative amount of  $\text{HD}_2\text{O}^+$  and  $\text{H}_2\text{DO}^+$  produced during the collision. A more accurate model for the process might also rationalize the difference in behavior found between the value of  $\mathcal{K}_{\text{MD}}$  and of the ratio  $k_{\text{exch}}/k_{\text{diss}}$  extracted from the analysis of the experimental data. We refer, in particular, to the fact that  $\mathcal{K}_{\text{exp}}$  becomes smaller than unity at  $E_{\text{int}} \sim 82$  kcal/mol,<sup>13</sup> whereas  $\mathcal{K}_{\text{MD}}$  remains substantially above unity over the explored energy range. We would like, however, to stress that a fair comparison with experimental results could only be made taking into account the probability of forming a complex as a function of the impact parameter, which cannot be addressed properly with our simulation protocol. Nevertheless, we feel that the details of the internal dynamics for  $\text{H}_5\text{O}_2^+$  provided by our numerical simulations are robust enough to warrant consideration in the analysis of experimental data.

The study presented in this paper has two possible shortcomings the impact of which is worth discussing. These are the use of classical MD simulations and of model potentials that somewhat underestimate the barrier for the exchange process with respect to high-level *ab initio* methods [see Fig. 1(a) for details and Ref. 13]. As for the latter, the difference in barrier height between the OSS2 and OSS3 TS's can be exploited to estimate the possible impact on the results. In this respect, it was found that the two sets of results were in quantitative agreement, suggesting that the phenomenon under study is not particularly sensitive to the fine details of the energy surface. This is important for the computational results and the associated theoretical analysis described in this work to provide appropriate guidelines for the interpretation of the experimental results on the title reaction, but it is clearly not so relevant if the attention is focused on discussing the occurrence and consequences of interesting nonstatistical effects in reaction dynamics. So, trajectories run on more accurate potential energy surfaces would certainly be useful to better clarify the impact of TS barrier heights, but it is nevertheless felt that the peculiar dynamics highlighted by the MD simulations is sufficiently robust to warrant consideration.

The issue of neglecting the quantum nature of the Zundel cation is slightly more problematic due to light hydrogen mass and the difficulties associated with testing the approximation involved in using classical MD. However, the good agreement between reduced-dimensionality quantum and



quasiclassical calculations of the proton exchange between H<sub>2</sub>O and H<sub>3</sub>O<sup>+</sup> (Ref. 14) suggests that quantum effects are not particularly important for this process, this being due to the attractive nature of the energy surface and the large amount of internal energy available to the collisional complex. Even so, the presence of tunneling effects, zero point motion, and the change in surface curvature along the exchange reaction path may somewhat modify the absolute value of the reaction constants. This, however, is likely to change only the quantitative details of the process, without eliminating the need for a dynamical description of the reactive process.

Although a bare proton is somewhat peculiar in nature, we believe that highly nonstatistical behavior should be expected for other ligand-exchange processes [e.g., H<sub>5</sub>O<sub>2</sub><sup>+</sup> plus D<sub>2</sub>O or Li<sup>+</sup>(H<sub>2</sub>O)<sub>*n*</sub> plus D<sub>2</sub>O]. These usually take place on strongly attractive surfaces characterized by many degenerate minima and that are likely to trap the collisional complex for long time. Investigation in this direction is already under way in our laboratory.

## ACKNOWLEDGMENTS

The author acknowledges Barry K. Carpenter, Peter J. Knowles, and Fausto Cargnoni for useful comments and Samuel R. Stone for a careful read of the manuscript. The authors also acknowledge financial support from EPSRC (GR/R77803/01).

<sup>1</sup>D. Townsend, S. A. Lahankar, S. K. Lee, S. D. Chambreau, A. G. Suits, X. Zhang, J. Rheinecker, L. B. Harding, and J. M. Bowman, *Science* **306**, 1158 (2004); L. Sun, K. Song, and W. L. Hase, *ibid.* **296**, 875 (2002); A. E. Pomerantz, J. P. Camden, A. S. Chiou, F. Ausfelder, N. Chawla, W. L. Hase, and R. N. Zare, *J. Am. Chem. Soc.* **127**, 16368 (2005); B. K. Carpenter, *J. Am. Chem. Soc.* **118**, 10329 (1996).

<sup>2</sup>D. L. Bunker and W. L. Hase, *J. Chem. Phys.* **59**, 4621 (1973).

<sup>3</sup>T. Baer and W. L. Hase, *Unimolecular Reaction Dynamics* (Oxford Uni-

versity Press, Oxford, 1996).

<sup>4</sup>M. Gruebele and P. G. Wolynes, *Acc. Chem. Res.* **37**, 261 (2004).

<sup>5</sup>V. Wong and M. Gruebele, *J. Phys. Chem. A* **103**, 10083 (1999).

<sup>6</sup>B. K. Carpenter, *J. Am. Chem. Soc.* **117**, 6336 (1995).

<sup>7</sup>M. B. Reyes and B. K. Carpenter, *J. Am. Chem. Soc.* **120**, 1641 (1998).

<sup>8</sup>P. W. Ryan, C. R. Blakley, M. L. Vestal, and J. H. Futrell, *J. Phys. Chem.* **84**, 561 (1980).

<sup>9</sup>D. Smith, N. G. Adams, and M. J. Henchman, *J. Chem. Phys.* **72**, 4951 (1980); N. G. Adams, D. Smith, and M. J. Henchman, *Int. J. Mass Spectrom. Ion Phys.* **42**, 11 (1982); M. J. Henchman, D. Smith, and N. G. Adams, *Int. J. Mass Spectrom. Ion Process.* **109**, 105 (1991).

<sup>10</sup>G. I. Mackay and D. K. Bohme, *J. Am. Chem. Soc.* **100**, 327 (1978); D. K. Bohme, G. I. Mackay, and S. D. Tanner, *ibid.* **101**, 3724 (1979).

<sup>11</sup>S. Yamaguchi, S. Kudoh, Y. Okada, T. Orii, K. Takeuchi, T. Ichikawa, and H. Nakai, *J. Phys. Chem. A* **107**, 10904 (2003).

<sup>12</sup>V. G. Anicich and A. D. Sen, *Int. J. Mass Spectrom. Ion Process.* **172**, 1 (1998).

<sup>13</sup>K. Honma and P. B. Armentrout, *J. Chem. Phys.* **121**, 8307 (2004).

<sup>14</sup>J. Rheinecker, T. Xie, and J. M. Bowman, *J. Chem. Phys.* **120**, 7018 (2004).

<sup>15</sup>M. Mella, *J. Chem. Phys.* **124**, 104302 (2006).

<sup>16</sup>L. Ojamäe, I. Shavitt, and S. J. Singer, *J. Chem. Phys.* **109**, 5547 (1998).

<sup>17</sup>M. Mella and A. Ponti, *ChemPhysChem* **7**, 894 (2006).

<sup>18</sup>M. Mella and D. C. Clary, *J. Chem. Phys.* **119**, 10048 (2003).

<sup>19</sup>H. W. Schranz, S. Nordholm, and B. C. Freasier, *Chem. Phys.* **108**, 69 (1986).

<sup>20</sup>H. W. Schranz, L. M. Raff, and D. L. Thompson, *J. Chem. Phys.* **94**, 4219 (1991).

<sup>21</sup>See EPAPS Document No. E-JCPA6-126-018722 for rate constants and time gap distributions obtained with OSS3, for semilogarithmic plots of the correlation functions, as well as for movies of trajectories. This document can be reached via a direct link in the online article's HTML reference section or via the EPAPS homepage (<http://www.aip.org/pubservs/epaps.html>).

<sup>22</sup>Even at the lowest energies explored by the experiments, only a small fraction (less than 10%) of trajectories was found undissociated after 10 ps.

<sup>23</sup>J. R. Beeler, Jr., *Phys. Rev.* **150**, 470 (1966).

<sup>24</sup>B. K. Carpenter, *Annu. Rev. Phys. Chem.* **56**, 57 (2005).

<sup>25</sup>Y. J. Cho, S. R. Vande Linde, L. Zhu, and W. L. Hase, *J. Chem. Phys.* **96**, 8275 (1992); L. Sun, W. L. Hase, and K. Song, *J. Am. Chem. Soc.* **123**, 5753 (2001).